Analysis and Purification Methods in Combinatorial Chemistry

Edited by

BING YAN

WILEY-INTERSCIENCE

A JOHN WILEY & SONS, INC., PUBLICATION

Analysis and Purification Methods in Combinatorial Chemistry

CHEMICAL ANALYSIS

A SERIES OF MONOGRAPHS ON ANALYTICAL CHEMISTRY
AND ITS APPLICATIONS

Editor
J. D. WINEFORDNER

VOLUME 163

Analysis and Purification Methods in Combinatorial Chemistry

Edited by

BING YAN

WILEY-INTERSCIENCE

A JOHN WILEY & SONS, INC., PUBLICATION

Published by John Wiley & Sons, Inc., Hoboken, New Jersey.
Published simultaneously in Canada.

Library of Congress Cataloging-in-Publication Data:
Analysis and purification methods in combinatorial chemistry / edited by Bing Yan.
p. cm.—(Chemical analysis; v. 1075)
Includes bibliographical references and index.
ISBN 0-471-26929-8 (cloth)
1. Combinatorial chemistry. I. Yan, Bing. II. Series.
RS419.A53 2004
615′.19—dc22

2003014606

Printed in the United States of America.

10 9 8 7 6 5 4 3 2 1

CONTENTS

PREFACE

More than 160 volumes of *Chemical Analysis: A Series of Monographs on Analytical Chemistry and Its Applications* have been published by John Wiley & Sons, Inc. since 1940. These volumes all focused on the most important analytical issues of their times. In the past decade one of the most exciting events has been the rapid development of combinatorial chemistry. This rapidly evolving field posed enormous analytical challenges early on. The two most-cited challenges are requirements for very high-throughput analysis of a large number of compounds and the analysis of polymer-bound compounds. Very impressive achievements have been made by scientists working in this field. However, there are still formidable analytical challenges ahead. For example, the development of highly parallel analysis and purification technologies and all methods associated with analysis to ensure combinatorial libraries are "synthesizable," "purifiable," and "drugable." For these evident reasons, I almost immediately agreed to edit a volume on the analysis and purification methods in combinatorial chemistry when the series editor Professor J. D. Winefordner asked me a year ago.

In the past year it has been a great pleasure for me to work with all contributors. The timely development of this volume is due entirely to their collaborative efforts. I have been impressed with their scientific vision and quality work throughout the year. To these contributors, I owe my very special thanks. I also owe a great debt to my colleagues especially Dr. Mark Irving, and Dr. Jiang Zhao for their assistance in my editorial work. Finally I wish to thank staff at Wiley for their professional assistance throughout this project.

Part I of the book includes six chapters describing various approaches to monitor reactions on solid support and optimize reactions for library synthesis: Lucas and Larive give a comprehensive overview of the principle and application of quantitative NMR analysis in support of synthesis in both solution and solid phase. Salvino describes in detail the application of ^{19}F NMR to monitor solid-phase synthesis directly on resin support. Cournoyer, Krueger, Wade, and Yan report on the single-bead FTIR method applied in monitoring solid-phase organic synthesis. Guinó and de Miguel report on HR-MAS NMR analysis of solid-supported samples.

A parallel analysis approach combined with chemometrics analysis in materials discovery and process optimization is presented by Potyrailo, Wroczynski, Lemmon, Flanagan, and Siclovan. Enjalbal, Lamaty, Martinez, and Aubagnac report their work on monitoring reactions on soluble polymeric support using mass spectrometry.

Part II of the book is dedicated to high-throughput analytical methods used to examine the quality of libraries. Hou and Raftery review the development of high-throughput NMR techniques and their own work on parallel NMR method. Simms details the theory and application of micellar electrokinetic chromatography as a high-throughput analytical tool for combinatorial libraries. Zhang and Fitch describe Affymax's approach on quality control and encoding/decoding of combinatorial libraries via single-bead analysis methods.

In Part III, various high-throughput purification techniques are discussed. Zhao, Zhang, and Yan review the chromatographic separation and their application in combinatorial chemistry. Hochlowski discusses various purification methods and the high-throughput HPLC and SFC methods developed at Abbott. God and Gumm present the new generation of parallel analysis and purification instruments and methods.

In Part IV, analytical methods applied in postsynthesis and postpurification stages are reviewed. Morand and Cheng report studies on stability profile of compound archives. Tseng, Chang, and Chu discuss a novel quartz crystal microbalance method to determine the binding between library compounds and biological targets. Faller reviews high-throughput methods for profiling compounds' physicochemical properties. Lipinski presents a detailed study of solubility issue in drug discovery and in combinatorial library design. Villena, Wlasichuk, Schmidt Jr., and Bao describe a high-throughput LC/MS method for the determination of $\log D$ value of library compounds.

BING YAN

August 2003
South San Francisco, California

CONTRIBUTORS

Jean-Louis Aubagnac, Laboratoire des aminocides, peptides et protéines, UMR 5810, Université de Montpellier II, 34095 Montpellier Cedex 5, France, E-mail: aubagnac@univ-montp2.fr

James J. Bao, Ph.D., Theravance, Inc., 901 Gateway Blvd., S. San Francisco, CA 94080, E-mail: jbao@theravance.com

I-Nan Chang, ANT Technology Co., Ltd., 7F-4, No. 134, Sec. 1, Fushing S Road, Taipei 106, Taiwan, ROC

Xueheng Cheng, Abbott Laboratories, Global Pharmaceutical Research and Development Division, Department R4PN, Building AP9A, 100 Abbot Park Road, Abbot Park IL 60064-6115, E-mail: xueheng.cheng@abbott.com

Yen-Ho Chu, Department of Chemistry, National Chung-Cheng University, Chia-Yi, Taiwan 621, Republic of China, E-mail: cheyhc@ccunix.ccu.edu.tw

Jason Cournoyer, ChemRx Division, Discovery Partners International, Inc., 385 Oyster Point Blve., South San Francisco, CA 94080

Yolanda de Miguel, Ph.D., Organic Chemistry Lecturer, Royal Society Dorothy Hodgkin Fellow, Chemistry Department, King's College London, Strand, London WC2R 2LS, E-mail: yolanda.demiguel@kcl.ac.uk

Christine Enjalbal, Laboratoire des aminocides, peptides et protéines, UMR 5810, Université de Montpellier II, 34095 Montpellier Cedex 5, France

Bernard Faller, Ph.D., Technology Program Head, Novartis Institute for Biomedical Research, WKL-122.P.33, CH-4002 Switzerland, Bernard.faller@pharma.novartis.com

William L. Fitch, Roche BioScience, Palo Alto, CA 94304

William P. Flanagan, General Electric, Combinatorial Chemistry Laboratory, Corporate Research and Development, PO Box 8, Schenectady, NY 12301-0008

Ralf God, Ph.D., Arndtstraß 2, D-01099 Dresden (Germany), E-mail: r.god@gmx.de

Meritxell Guinó, Organic Chemistry Lecturer, Royal Society Dorothy Hodgkin Fellow, Chemistry Department, King's College London, Strand, London WC2R 2LS

Holger Gumm, SEPIAtec GmbH, Louis-Bleriot-Str. 5, D-12487 Berlin, Germany, E-mail: hgumm@sepiatec.com

Jill Hochlowski, Abbott Laboratories, Dept. 4CP, Bldg. AP9B, 100 Abbott Park Road, Abbott Park, IL 60064-3500, E-mail: Jill.hochlowski@abbott.com

Ting Hou, Department of Chemistry, West Lafayette, IN 47907-1393

Clinton A. Krueger, ChemRX Division, Discover Partners International, Inc., South San Francisco CA 94080

Cynthia K. Larive, University of Kansas, Department of Chemistry, 2010 Malott Hall, 1251 Wescoe Hall Rd, Lawrence, KS 66045, E-mail: clarive@ku.edu

Frederic Lamaty, Laboratoire des aminocides, peptides et protéines, UMR 5810, Université de Montpellier II, 34095 Montpellier Cedex 5, France, E-mail: frederic@ampir1.univ-montp2.fr

John P. Lemmon, General Electric, Combinatorial Chemistry Laboratory, Corporate Research and Development, PO Box 8, Schenectady, NY 12301-0008

Christopher A. Lipinski, Ph.D., Pfizer Global R&D, Groton Labs, Eastern Point Road, MS 8200-36, Groton, CT 06340, E-mail: christopher_a_lipinski@groton.pfizer.com

Laura H. Lucas, Dept of Chemistry, 2010 Malott Hall, University of Kansas, Lawrence KS 66045

J. Martinez, Laboratoire des aminocides, peptides et protéines, UMR 5810, Université de Montpellier II, 34095 Montpellier Cedex 5, France, E-mail: mlorca@univ-montp2.fr

Kenneth Morand, Procter & Gamble Pharmaceuticals, Health Care Research Center, 8700 Mason-Montgomery Road, Mason, OH 45040, E-mail: morand.kl@pg.com

Radislav A. Potyrailo, General Electric, Combinatorial Chemistry Laboratory, Corporate Research and Development, PO Box 8, Schenectady, NY 12301-0008, E-mail: potyrailo@crd.ge.com

Daniel Raftery, Department of Chemistry, West Lafayette, IN 47907-1393, E-mail: raftery@purdue.edu

Joseph M. Salvino, Ph.D., Rib-X Pharmaceuticals, Inc., 300 George St., New Haven, CT 06511, E-mail: jsalvino@Rib-x.com

Donald E. Schmidt, Jr., Theravance, Inc., 901 Gateway Blvd., S. San Francisco, CA 94080

Oltea P. Siclovan, General Electric, Combinatorial Chemistry Laboratory, Corporate Research and Development, PO Box 8, Schenectady, NY 12301-0008

Peter J. Simms, Ribapharm Inc., 3300 Hyland Ave., Costa Mesa, CA 92626, E-mail: pjsimms@icnpharm.com

Ming-Chung Tseng, Dept of Chemistry and Biochemistry, National Chung Cheng University, 160 San-Hsing, Min-Hsiung, Chia-Yi 621, Taiwan, ROC

Jenny D. Villena, Theravance, Inc., 901 Gateway Blvd., S. San Francisco, CA 94080

Janice V. Wade, ChemRX Division, Discover Partners International, Inc., South San Francisco CA 94080

Ken Wlasichuk, Theravance, Inc., 901 Gateway Blvd., S. San Francisco, CA 94080

Ronald J. Wroczynski, General Electric, Combinatorial Chemistry Laboratory, Corporate Research and Development, PO Box 8, Schenectady, NY 12301-0008

Bing Yan, ChemRX Division, Discover Partners International, Inc., South San Francisco CA 94080, E-mail: byan@chemrx.com

Jing Jim Zhang, Ph.D., Affymax, Inc., 4001 Miranda Avenue, Palo Alto, CA 94304, E-mail: jim_zhang@affymax.com

Lu Zhang, ChemRx Division, Discovery Partners International, Inc., 9640 Towne Centre Drive, San Diego, CA 92121

Jiang Zhao, ChemRx Division, Discovery Partners International, Inc., 385 Oyster Point Blve., South San Francisco, CA 94080, E-mail: jzhao@chemrx.com

PART

I

ANALYSIS FOR FEASIBILITY AND OPTIMIZATION OF LIBRARY SYNTHESIS

CHAPTER

1

QUANTITATIVE ANALYSIS IN ORGANIC SYNTHESIS WITH NMR SPECTROSCOPY

LAURA H. LUCAS and CYNTHIA K. LARIVE

1.1. INTRODUCTION

The development of combinatorial methods of synthesis has created a great need for robust analytical techniques amenable to both small- and large-scale syntheses as well as high-throughput analysis. A variety of spectroscopic methods such as mass spectrometry (MS), infrared spectroscopy (IR), and nuclear magnetic resonance (NMR) spectroscopy have been widely used in the combinatorial arena.[1–4] Many of these methods have been coupled online with high-performance liquid chromatography (HPLC), and such hyphenated techniques afford high-resolution structural data on library compounds.[5–7] NMR has an advantage over other spectroscopic techniques because it is a universal analytical method that potentially reveals the identity and purity of any organic compound. Since organic molecules contain ^{1}H and ^{13}C, nuclei that are NMR active, no analyte derivitization is necessary. NMR can also distinguish isomers or structurally similar compounds that may coelute when analyzed by HPLC. This selectivity is especially important when attempting to resolve and quantitate structures of library compounds or natural products.[8] Furthermore the noninvasive nature of NMR allows the sample to be recovered for additional analyses or used in a subsequent reaction.

Although traditionally thought of as a low-sensitivity technique, technological improvements in NMR instrumentation have significantly reduced sample mass requirements and experiment times. Sensitivity enhancements have been achieved with higher field magnets, small-volume flow probes for solution-phase analysis,[9] the introduction of cryogenically cooled NMR receiver coils and preamplifiers,[10–13] and high-resolution magic-angle spinning (HR-MAS) NMR technology for solid-phase systems, making routine analysis of μg quantities (or less) possible.[14,15] These advancements com-

Analysis and Purification Methods in Combinatorial Chemistry, Edited by Bing Yan.
ISBN 0-471-26929-8

bined with developments in automated sample handling and data processing have improved the throughput of NMR such that entire 96-well microtitre plates can be analyzed in just a few hours.[16]

Besides the structural information provided by NMR, quantitation is possible in complex mixtures even without a pure standard of the analyte, as long as there are resolved signals for the analyte and reference compound. This is a particular advantage in combinatorial chemistry, where the goal is the preparation of large numbers of new compounds (for which no standards are available). Since the NMR signal arises from the nuclei (e.g., protons) themselves, the area underneath each signal is proportional to the number of nuclei. Therefore the signal area is directly proportional to the concentration of the analyte:

$$\frac{\text{Area}}{\text{Number of nuclei}} \propto \text{Concentration} \tag{1.1}$$

This relationship holds true when experimental parameters are carefully optimized, which may require some additional experimental time.

Consider the example shown in Figure 1.1 for the quantitation of a maleic acid solution, containing a known concentration of the primary standard potassium hydrogen phthalate (KHP). A primary analytical standard is a material of very high purity for which the mass of the compound can be used directly in the calculation of solution concentration. The area of the KHP peak is divided by 4.0, the number of protons that contribute to the KHP aromatic resonances, so that its normalized area is 1773.1. Similarly the maleic acid peak area is normalized by dividing by 2.0 to give a normalized area of 1278.3. A simple proportion can then be established to solve for the concentration of maleic acid:

$$\frac{\text{Normalized area}_{(\text{Maleic acid})}}{[\text{Maleic acid}]} = \frac{\text{Normalized area}_{(\text{KHP})}}{[\text{KHP}]},$$

$$[\text{Maleic acid}] = \frac{[\text{KHP}] \times \text{Normalized area}_{(\text{Maleic acid})}}{\text{Normalized area}_{(\text{KHP})}},$$

$$[\text{Maleic acid}] = \frac{28.5\,\text{mM} \times 1278.3}{1773.1},$$

$$[\text{Maleic acid}] = 28.5\,\text{mM} \times 0.72094.$$

The concentration of maleic acid in this solution is therefore about 72% that of the primary standard KHP. In this example the concentration of the KHP is 28.5 mM and the calibrated concentration of maleic acid is 20.5 mM. Even though maleic acid is not a primary standard, this standardized maleic

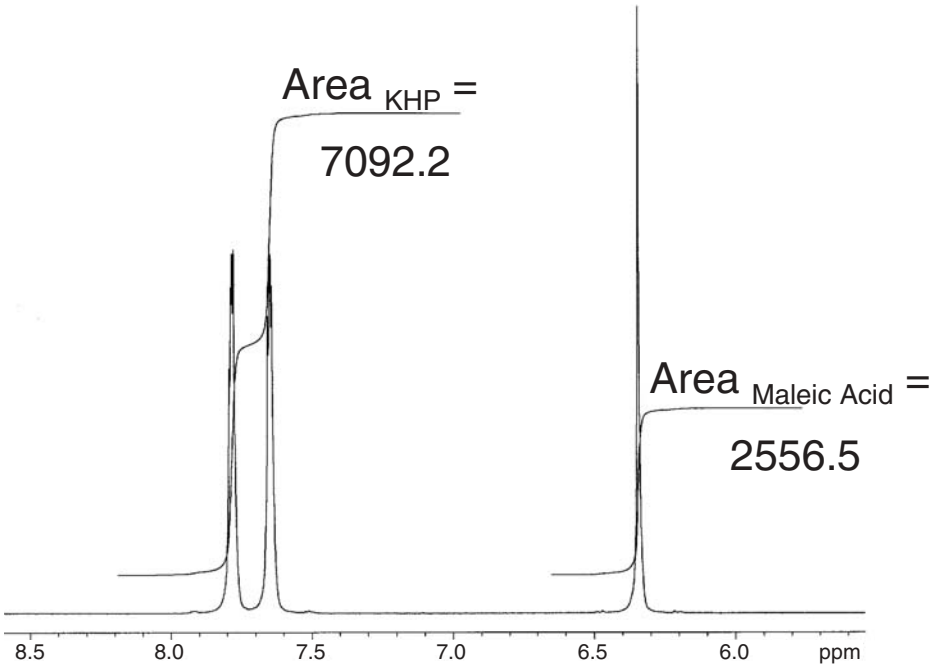

Figure 1.1. 600 MHz ^{1}H NMR spectrum of potassium hydrogen phthalate (KHP) and maleic acid dissolved in D_2O. The KHP is a primary standard by which the maleic acid concentration can be quantitated. The data represents 8 FIDs coadded into 28,800 points (zero-filled to 32K points) across a spectral width of 7200.1 Hz. An exponential multiplier equivalent to 0.5 Hz line broadening was then applied.

acid solution can now be used to quantitate additional samples in a similar manner (e.g., ibuprofen as discussed in more detail below). This approach allows the selection of a quantitation standard based on its NMR spectral properties and does not require that it possess the properties of a primary analytical standard.

1.2. FUNDAMENTAL AND PRACTICAL ASPECTS OF THE QUANTITATIVE NMR EXPERIMENT

1.2.1. Experimental Parameters

For a detailed description of NMR theory and practice, the reader is encouraged to see one of the many excellent books on the subject.[17–20] A brief description of the NMR experiment is presented below, with an emphasis

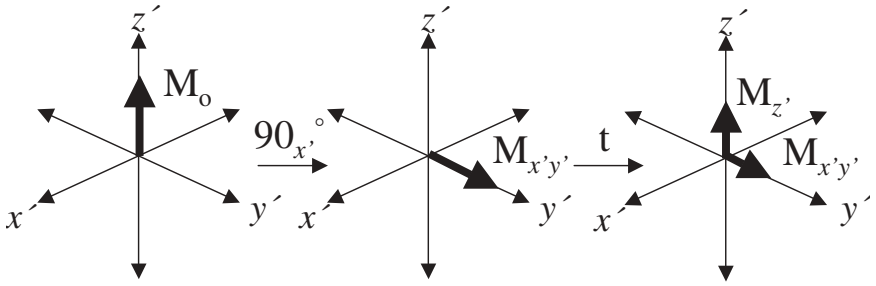

Figure 1.2. The equilibrium population difference of the nuclei in an applied magnetic field can be represented as a vector $\mathbf{M}_o$. Disturbing this macroscopic magnetization away from its equilibrium position creates the NMR signal. This is accomplished by application of a radio frequency pulse (90° along the x' axis in this example) to tip the magnetization into the $x'y'$ plane of the rotating frame of reference. During a time delay t, following the pulse the detectable magnetization $\mathbf{M}_{x'y'}$, decays by T_2 relaxation in the transverse plane while the longitudinal magnetization $\mathbf{M}_{z'}$ begins to recover through T_1 relaxation.

on the important parameters for proper acquisition and interpretation of spectra used for quantitation. When the sample is placed in the magnetic field, the nuclei align with the field, by convention along the z' axis in the rotating frame of reference, as illustrated in Figure 1.2 by the vector, $\mathbf{M}_o$, representing the macroscopic magnetization. A radio frequency pulse (B_1) applied for time t_p tips the magnetization through an angle, θ:

$$\theta = \gamma B_1 t_p, \tag{1.2}$$

where γ is the gyromagnetic ratio of the nucleus of interest. A 90° radio frequency (rf) pulse along the x' axis tips the magnetization completely into the $x'y'$ plane to generate the observable signal, $\mathbf{M}_{x'y'}$. After the pulse the magnetization will relax back to equilibrium via two mechanisms: spin-spin (T_2, transverse) relaxation and spin-lattice (T_1, longitudinal) relaxation. This is shown in Figure 1.2 as a decrease in the magnitude of the $x'y'$ component of the vector $\mathbf{M}_o$ and an increase in the magnitude of the z' component at time t following the pulse. Acquisition of $\mathbf{M}_{x'y'}$ for all nuclei in the sample as a function of time results in the free induction decay (FID), which upon Fourier transformation is deconvolved into the frequency domain and displayed as the familiar NMR spectrum. The FID decays exponentially according to T_2, the spin-spin or transverse relaxation time. In addition to the natural T_2 relaxation times of the nuclei that comprise the FID, magnetic field inhomogeneity contributes to the rate at which the transverse magnetization is lost. The apparent transverse relaxation time, T_2^*, is the summation of the natural relaxation time and the component induced by

magnetic field inhomogeniety and can be calculated from the width at half-height of the NMR signals:

$$w_{1/2} = \frac{1}{\pi T_2^*}. \tag{1.3}$$

The acquisition time during which the FID is detected is often set to three to five times T_2^* to avoid truncation of the FID.

1.2.2. T_1 Relaxation

Just as the NMR signal decays exponentially in the transverse plane, the magnetization also relaxes back to its equilibrium state in an exponential fashion during the time t following the rf pulse. For the longitudinal component ($\mathbf{M}_{z'}$), this occurs as a first-order rate process:

$$\mathbf{M}_{z'} = \mathbf{M}_o\left[1 - \exp\left(\frac{-t}{T_1}\right)\right]. \tag{1.4}$$

Equation (1.4) reveals that when the magnetization is fully tipped into the $x'y'$ plane by a 90° pulse, the magnetization will recover to 99.3% of its equilibrium value along z' at $t = 5T_1$. The T_1 relaxation time can be measured with an inversion-recovery experiment,[21] where a 180° pulse inverts the magnetization to the negative z' axis and allows the magnetization to recover for various times until the curve described by Eq. (1.5) is adequately characterized:

$$\mathbf{M}_{z'} = \mathbf{M}_o\left[1 - 2\exp\left(\frac{-t}{T_1}\right)\right]. \tag{1.5}$$

Equation (1.5) is equivalent to (1.4), except the factor of 2 reflects the use of a 180° pulse, meaning that the magnetization (signal intensity) now should take twice as long to recover as when a 90° pulse is used. The results of the inversion-recovery experiment are illustrated in Figure 1.3, where the recovery of ibuprofen and maleic acid resonances are shown as a series of spectra and as signal intensities (inset) fit to Eq. (1.5).

It should be noted that if the sample contains multiple components, the 90° pulse will not be exactly the same for all spins. Equations (1.3) to (1.5) will not hold rigorously, leading to errors in T_1 measurements. Correction factors can be performed mathematically[22] or by computer simulation,[23] depending on the complexity of the sample. In practice, the average 90° pulse or the 90° pulse for the peaks of interest is used.

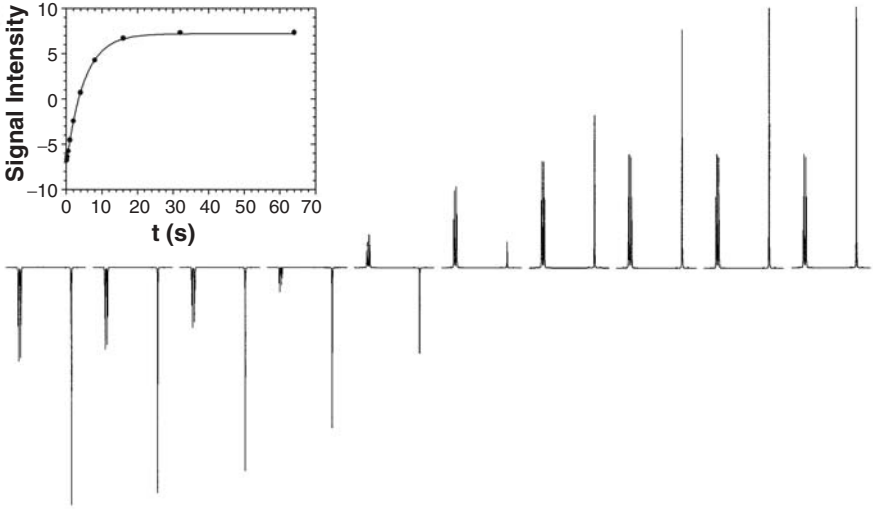

Figure 1.3. Inversion-recovery experimental results for determining T_1 relaxation times of ibuprofen and maleic acid. The spectral region from 5.6 to 7.6 ppm is displayed as a function of the variable delay time t. The t values used were (from left to right across the figure): 0.125 s, 0.25 s, 0.50 s, 1.0 s, 2.0 s, 4.0 s, 8.0 s, 16 s, 32 s, and 64 s. The acquisition and processing parameters are the same as for Figure 1.1. The inset shows the signal intensities of the maleic acid peak (5.93 ppm) fit to Eq. (1.5).

1.2.3. Repetition Time

As mentioned previously, the T_1 relaxation time affects the repetition time (acquisition time + relaxation delay), which must be carefully chosen to ensure that the magnetization returns to equilibrium between pulses. If the time between FIDs is insufficient to allow for complete relaxation, the intensity of the detected magnetization will be reduced:

$$\mathbf{M}_{x'y'} = \frac{\mathbf{M}_o\left[1-\exp\left(\frac{-t_r}{T_1}\right)\right]\sin\theta}{\left[1-\exp\left(\frac{-t_r}{T_1}\right)\right]\cos\theta}, \tag{1.6}$$

where t_r is the repetition time and θ is the tip angle.[24] If the sample contains multiple components, t_r should be set based on the longest T_1 measured for results to be fully quantitative. The ^{1}H spectrum in Figure 1.4 for an ibuprofen-maleic acid mixture measured using an average 90° pulse shows that the ibuprofen T_1 relaxation times range from 0.721 to 2.26 s, but maleic acid

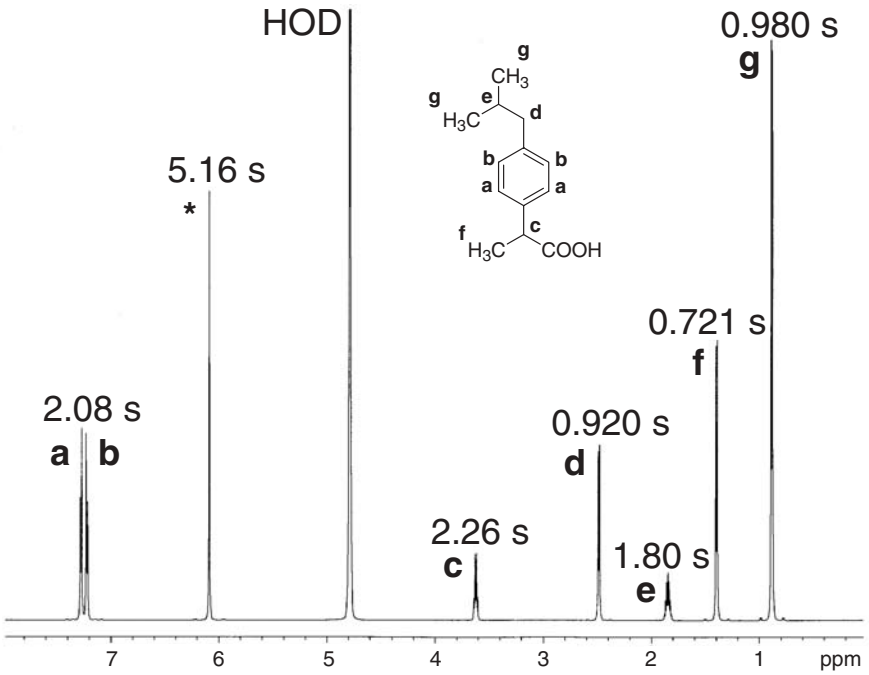

Figure 1.4. 600 MHz ^{1}H NMR spectrum of the ibuprofen-maleic acid mixture. The average T_1 relaxation times are displayed above each peak. The asterisk (*) indicates the maleic acid peak while the ibuprofen peaks are labeled *a* to *g* to correspond with the structure. The acquired data were zero-filled to 32 K, and other acquisition and processing parameters are as listed for Figure 1.1.

has a T_1 of 5.16 s. Therefore, to quantitate the ibuprofen concentration using the internal standard maleic acid, the repetition time should be >25 s if a 90° pulse is used. Because multiple relaxation mechanisms exist (e.g., dipole-dipole interactions, chemical shift anisotropy, and spin-rotation relaxation),[17] T_1 values for different functional groups may vary significantly, as illustrated by ibuprofen.

The consequences of a truncated repetition time are shown in Figure 1.5 for the ibuprofen aromatic protons and maleic acid singlet. Repetition times of 0.7, 1, 3, and $5T_1$ (based on the measured T_1 of maleic acid, 5.16 s) were used. The intensities of the ibuprofen aromatic proton resonances are less affected by decreased repetition times, since their T_1 values are much shorter, and appear to have recovered fully when a repetition time of $3T_1$ (15.5 s) is used. The intensity of the maleic acid singlet is more significantly affected because its T_1 is longer. The integral of the maleic acid resonance

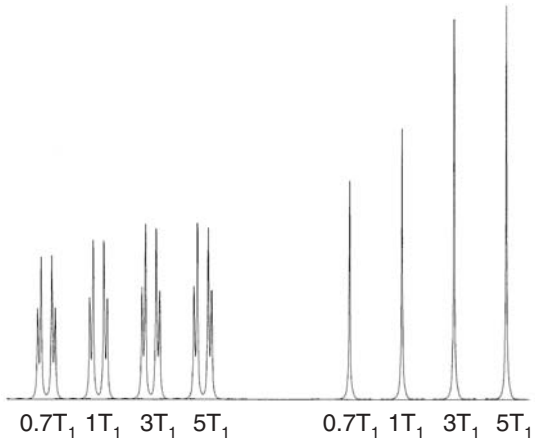

Figure 1.5. ^{1}H spectra for the ibuprofen-maleic acid mixture acquired with different repetition times. Only the spectral region including the aromatic ibuprofen protons and maleic acid singlet is shown. The repetition times were selected on the basis of the measured T_1 of maleic acid (5.16 s) and are as follows: $0.7T_1$ (3.57 s), $1T_1$ (5.16 s), $3T_1$ (15.5 s), and $5T_1$ (25.8 s). All spectra were acquired and processed as described for Figure 1.1.

is the basis for the quantitation of the ibuprofen concentration, and repetition times shorter than $5T_1$ lead to reduced integral values for maleic acid. This results in positive systematic errors in the calculated ibuprofen concentration as shown in Table 1.1. The quantitation errors are greater when shorter repetition times are used, resulting in a gross overestimation of the ibuprofen concentration.

To efficiently utilize instrument time, it may be necessary to use repetition times less than $5T_1$. Theoretically the signal intensities obtained using a repetition time less than $5T_1$ should be correctable according to Eq. (1.1). For example, the data acquired with a repetition time of $1T_1$ (5.16 s) should give a maleic acid signal that is 63.2% recovered. The ibuprofen aromatic proton signals are 91.6% recovered at this repetition time because of their faster T_1 recovery. The signal areas can be corrected to determine their value at 100% recovery. Using the corrected integrals, an ibuprofen concentration of 50.4 mM was obtained. This result reflects an approximate 10% error relative to the fully relaxed data (acquired with a repetition time of $5T_1$) and may result from pulse imperfections as well as T_1 differences for the two ibuprofen aromatic protons (which were not completely baseline resolved and hence integrated together). These results show that the repetition time is probably the most important experimental parameter in

Table 1.1. Quantitation Accuracy of Ibuprofen against Maleic Acid as an Internal Standard Using Various Repetition Times and Tip Angles

Repetition Time	Tip Angle (°)	[Ibuprofen] (mM)	Measured Error[a]
$5T_1$ (25.8 s)	90	56.6	N/A[b]
$3T_1$ (15.5 s)	90	58.0	2.5%
$1T_1$ (5.16 s)	90	73.0	29.0%
$1T_1$ (5.16 s)	51	63.1	11.5%
$0.7T_1$ (3.57 s)	90	80.5	42.2%

[a] Measured errors in concentration were determined relative to the fully relaxed spectrum acquired with a repetition time of $5T_1$.
[b] Not applicable.

quantitation by NMR, and that proper quantitation can take time. (The fully relaxed spectrum was acquired in 27.5 minutes.)

1.2.4. Signal Averaging

Proper quantitation may require even longer experimental times when a limited amount of sample is available and signal averaging is necessary to improve the spectral signal-to-noise ratio (S/N). Coherently adding (coadding) successive single-pulse experiments increases the S/N by a factor of $\sqrt{N}$, where N is the number of FIDs added together. This is shown by the improvements in the spectral S/N in Figure 1.6 for the ibuprofen and maleic acid spectra as more FIDs are coadded. As shown in Table 1.2, the increases in S/N observed for increasing numbers of FIDs are very close to those predicted. The quantitation precision is not significantly affected by the number of FIDs co-added in this example, since both components are present at fairly high (millimolar) concentrations. However, the precision with which resonance intensities are determined directly depends on the error in the integrals. Therefore the precision of concentration determinations may be limited by the spectral S/N for more dilute solutions unless signal averaging is employed.

The signal intensity lost due to incomplete relaxation when repetition times less than $5T_1$ are used can often be regained by signal-averaging.[25] As shown by Rabenstein, when a 90° tip angle is used, S/N reaches a maximum when the repetition time is $1.25T_1$ (compared to using a $5T_1$ repetition time in an equivalent total experimental time).[24,26] The S/N is affected by both the repetition time and the tip angle. A tip angle less than 90° generates less signal (since the magnetization is not fully tipped into the $x'y'$ plane),

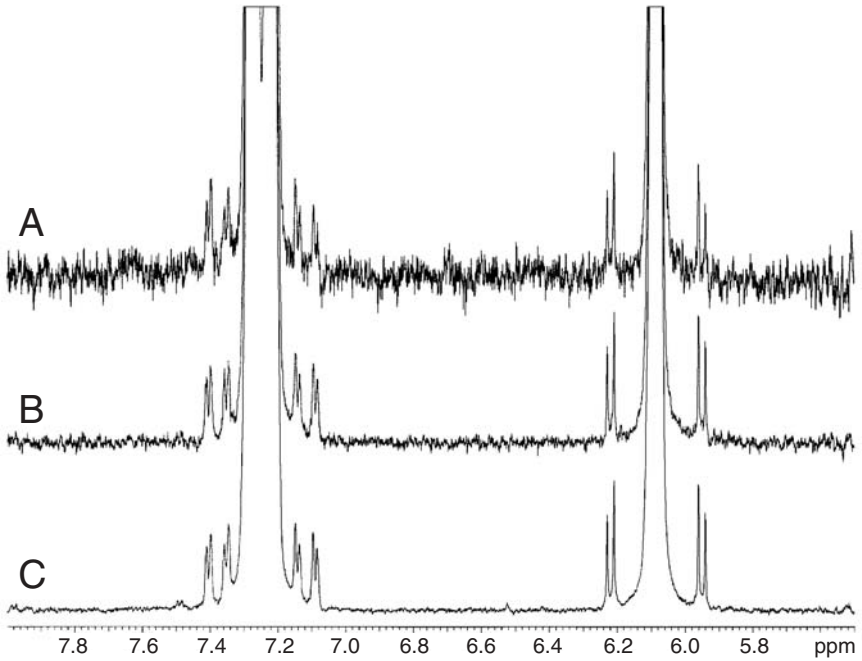

Figure 1.6. [1]H spectra for the ibuprofen-maleic acid mixture acquired with 1 (*A*), 8 (*B*), and 64 (*C*) FIDs coadded to improve the spectral signal-to-noise ratio (*S*/*N*). Again, only the ibuprofen aromatic and maleic acid peaks are displayed. The actual *S*/*N* values for each spectrum are shown in Table 1.2. Acquisition and processing parameters match those given for Figure 1.1.

Table 1.2. Improvements in the Signal-to-Noise Ratio (*S*/*N*) Gained by Co-adding Successive FIDs for Ibuprofen (IB) and Maleic Acid (MA)

Number of FIDs	*S*/*N* IB	*S*/*N* MA	Predicted *S*/*N* Increase	Actual *S*/*N* Increase IB	Actual *S*/*N* Increase MA	Concentration IB
1	987.3	2,041.7	N/A[a]	N/A[a]	N/A[a]	56.9 mM
8	2,737.5	6,450.3	2.83[b]	2.77[b]	3.16[b]	56.5
64	7,164.8	17,358	8.00[b]	7.26[b]	8.50[b]	56.6

[a] Not applicable.
[b] Calculated relative to the result for 1 FID.

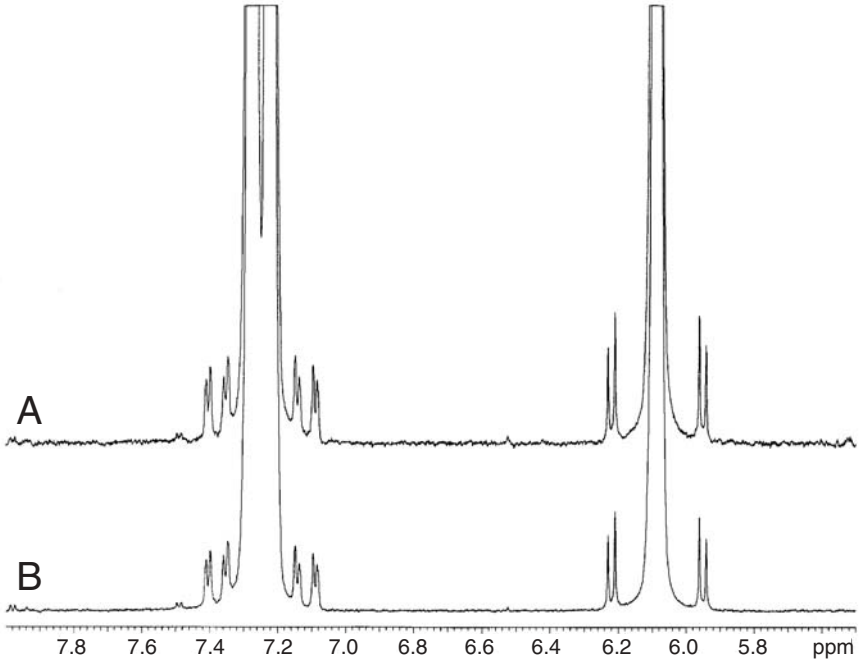

Figure 1.7. ^{1}H NMR spectra for the ibuprofen-maleic acid mixture acquired in 27.5 minutes. Spectrum (*A*) was acquired with 64 FIDs and a repetition time of $5T_1$ (25.8 s), using a 90° tip angle. Spectrum (*B*) was acquired with 320 FIDs and a repetition time of $1T_1$ (5.16 s), with a 50.8° tip angle as calculated by Eq. (1.7).

but less time is required for the magnetization to relax to equilibrium, affording more time for signal averaging. If the T_1 of the analyte and desired repetition time are known, the optimum tip angle (i.e., the Ernst angle) is calculated with

$$\cos\theta = \exp\left(\frac{-t}{T_1}\right). \tag{1.7}$$

Using the known T_1 of maleic acid (5.16 s) and a desired repetition time of $1T_1$, the Ernst angle calculated for this solution is 50.8°. Figure 1.7 shows the improved *S*/*N* achieved when a shorter tip angle is used. Spectrum A represents 64 FIDs acquired with a 90° pulse and a repetition time of $5T_1$. The total experimental time was 27.5 minutes. When a 50.8° pulse and $1T_1$ repetition time were used, 320 FIDs could be co-added in an equivalent experimental time (Figure 1.7*B*). The S/N ratios achieved by acquiring 320

FIDs with a reduced tip angle increased by a factor of 1.74 for ibuprofen and 1.54 for maleic acid relative to the *S*/*N* obtained with 64 FIDs and a 90° tip angle. This is again attributed to the differences in T_1 for the two molecules and leads to an inflated ibuprofen concentration (63.1 mM compared to 56.6 mM). While the error might be less if the T_1 relaxation times are nearly the same for the standard and the analyte, in many quantitation experiments a 90° tip angle and repetition time of $\geq 5T_1$ are used, especially if extensive signal averaging is not required.[26]

1.2.5. Defining Integrals

When considering the inversion-recovery experiment, it is illustrative to monitor the exponential recovery of signal intensity. However, relative peak heights vary based on their widths and shapes, so peak areas must be measured for quantitation.[26] Because NMR signals exhibit Lorentzian lineshapes, the peaks theoretically extend to infinity on either side of the actual chemical shift. Given that the peaks are phased properly and digital resolution is sufficient, Rabenstein has reported that 95% of the Lorentzian peak area can be described if the integral region encompasses 6.35 times the line width at half-height.[26] In most cases this will be impractical since other resonances will be present in this frequency range. But does it make a difference how wide the integral regions are? Figure 1.8 shows the integrals determined for ibuprofen and maleic acid using three different methods: truncating the integrals on either side of the main peak, truncating the integrals where the ^{13}C-satellites are baseline resolved, and extending the integral regions on either side of the peak so that the total region integrated is three times the width between the ^{13}C satellites. Table 1.3 shows that including ^{13}C satellites does make a small difference in the peak areas but extending the integral regions past the satellites does not. This result is not surprising, especially if baseline correction is applied near the peaks that may truncate the Lorentzian line shapes. As shown in Table 1.3, failing to apply baseline correction results in significant errors in quantitation (10% in this example) when wider integral regions are used. Since line widths are not constant for all peaks, it is important to define integral regions based on individual line widths rather than a fixed frequency range.[26] For example, if a constant integral region of 92 Hz is used to quantitate the example shown in Figure 1.8, the resulting ibuprofen concentration is 56.6 mM. Since the ibuprofen and maleic acid peaks have similar line widths in this example, the resulting concentration is not drastically affected. Significantly different results could be expected if products tethered to solid-phase resins were analyzed, since the heterogeneity of the